Report

Current Biology

# Distributed Plasticity Drives Visual Habituation Learning in Larval Zebrafish

## Graphical Abstract

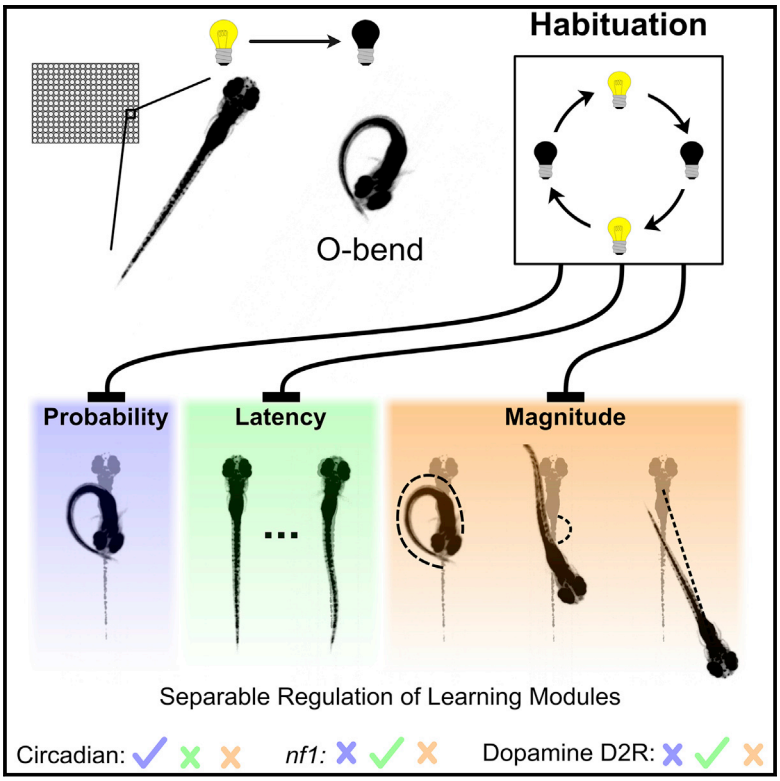


## Authors

Owen Randlett, Martin Haesemeyer, Greg Forkin, Hannah Shoenhard, Alexander F. Schier, Florian Engert, Michael Granato

## Correspondence

owen.randlett@gmail.com (O.R.), florian@mcb.harvard.edu (F.E.), granatom@pennmedicine.upenn.edu (M.G.)

## In Brief

Animals habituate to repeated stimuli, learning to ignore potential distractions. Randlett et al. show that multiple components of the larval zebrafish dark-flash response habituate independently using different molecular mechanisms. This reveals that habituation learning is a modular process that selectively adapts specific components of behavior.

## Highlights

- High-throughput behavioral analysis of dark-flash habituation in larval zebrafish
- Multiple components of the response adapt with different habituation kinetics
- Controlled by multiple circuit loci with different molecular requirements
- Modular habituation selectively tunes behavioral components based on context

Randlett et al., 2019, Current Biology *29*, 1–9
April 22, 2019 
https://doi.org/10.1016/j.cub.2019.02.039

CellPress

Please cite this article in press as: Randlett et al., Distributed Plasticity Drives Visual Habituation Learning in Larval Zebrafish, Current Biology (2019), https://doi.org/10.1016/j.cub.2019.02.039

Current Biology
Report

# Distributed Plasticity Drives Visual Habituation Learning in Larval Zebrafish

Owen Randlett,[1,2,*] Martin Haesemeyer,[2] Greg Forkin,[1] Hannah Shoenhard,[1] Alexander F. Schier,[2,3,4,5,6] Florian Engert,[2,3,7,*] and Michael Granato[1,7,8,*]
[1]Department of Cell and Developmental Biology, University of Pennsylvania Perelman School of Medicine, Philadelphia, PA 19104, USA
[2]Department of Molecular and Cellular Biology, Harvard University, Cambridge, MA 02138, USA
[3]Center for Brain Science, Harvard University, Cambridge, MA 02138, USA
[4]Broad Institute of MIT and Harvard, Cambridge, MA 02142, USA
[5]Harvard Stem Cell Institute, Cambridge, MA 02138, USA
[6]Biozentrum, University of Basel, 4056 Basel, Switzerland
[7]Senior author
[8]Lead Contact
*Correspondence: owen.randlett@gmail.com (O.R.), florian@mcb.harvard.edu (F.E.), granatom@pennmedicine.upenn.edu (M.G.)
https://doi.org/10.1016/j.cub.2019.02.039

## SUMMARY

Habituation is a simple form of learning where animals learn to reduce their responses to repeated innocuous stimuli [1]. Habituation is thought to occur via at least two temporally and molecularly distinct mechanisms, which lead to short-term memories that last for seconds to minutes and long-term memories that last for hours or longer [1, 2]. Here, we focus on long-term habituation, which, due to the extended time course, necessitates stable alterations to circuit properties [2–4]. In its simplest form, long-term habituation could result from a plasticity event at a single point in a circuit, and many studies have focused on identifying the site and underlying mechanism of plasticity [5–10]. However, it is possible that these individual sites are only one of many points in the circuit where plasticity is occurring. Indeed, studies of short-term habituation in *C. elegans* indicate that in this paradigm, multiple genetically separable mechanisms operate to adapt specific aspects of behavior [11–13]. Here, we use a visual assay in which larval zebrafish habituate their response to sudden reductions in illumination (dark flashes) [14, 15]. Through behavioral analyses, we find that multiple components of the dark-flash response habituate independently of one another using different molecular mechanisms. This is consistent with a modular model in which habituation originates from multiple independent processes, each adapting specific components of behavior. This may allow animals to more specifically or flexibly habituate based on stimulus context or internal states.

## RESULTS

### High-Throughput Quantification of Dark-Flash Habituation

When exposed to a sudden transition to whole-field darkness (dark flash), larval zebrafish startle. These startles are characterized by a large-angle body bend followed by a swim forward in the new direction (Figure 1A; Video S1) [16]. These movements were originally classified as "O-bend" maneuvers, but a recent behavioral clustering analysis indicates that a second kinematically distinct movement termed a spot avoidance turn (SAT) can also be elicited by dark flashes [17]. Although the neural circuitry underlying the dark-flash response has not been well described, it is known to be retina dependent [18]. At the reticulospinal level, the dark-flash response does not require the Mauthner neuron that drives the acoustic escape response [16] but does require the smaller and more ventromedially located reticulospinal neurons that also drive spontaneous turning behaviors (RoV3, MiV1, and MiV2) [19, 20]. Importantly, larval zebrafish exhibit protein-synthesis-dependent long-term habituation to dark flashes, which, similar to memory formation in *Drosophila* and mice, requires neurofibromatosis 1 (Nf1)-dependent cyclic AMP (cAMP)- and Ras-mediated plasticity [15, 21, 22].

We developed a high-throughput behavioral setup that can track 600 larvae in individual wells, deliver visual and acoustic stimuli, and track stimulus responses at 560 Hz (Figure 1B; see STAR Methods). This allows us to maintain individual larval identity throughout the experiment, to monitor behavior over days, and to unambiguously classify stimulus responses using postural reconstruction of the bending axis of the larvae. Adapting an established dark-flash habituation assay [14, 15], we developed a paradigm that consists of 4 training blocks of 60 dark flashes at 1-min interstimulus intervals, with blocks separated by 62 min of rest. This spaced training paradigm induced habituation, which we quantified as the progressively decreasing probability of executing a dark-flash response (Figures 1B and 1C; Video S2). Fitting curves to each block with an exponential function (Figure 2A) revealed that, after each rest period, the

Please cite this article in press as: Randlett et al., Distributed Plasticity Drives Visual Habituation Learning in Larval Zebrafish, Current Biology (2019), https://doi.org/10.1016/j.cub.2019.02.039



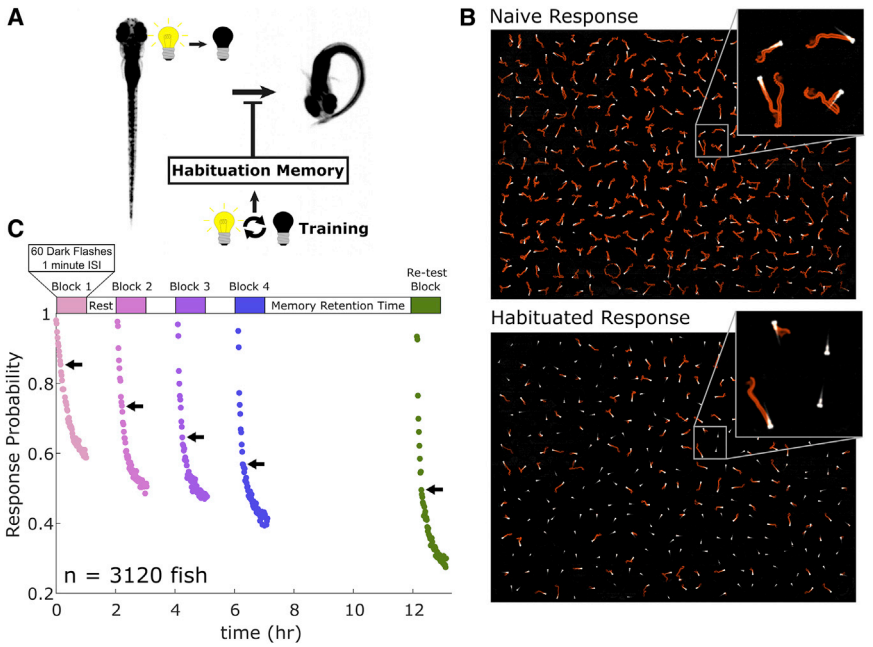


**Figure 1. Habituation of the Dark-Flash Response**

(A) When stimulated with a dark flash, larval zebrafish execute a high-amplitude turn, which habituates with training [14].

(B) Time projection images from a 0.9-s recording of the same 300 larvae for the first flash (naive response) and the 240$^{th}$ flash (habituated response). Motion is visible as orange streaks in the image, tracing the path traveled by the larvae. Larvae that do not move are visible as stationary white larvae (insets). Larvae were recorded in 300-well plates, and images were background subtracted to remove the behavior plates.

(C) The response probability across the population of larvae decreased both within the 60-flash training blocks and successively across the 4 blocks of training. Each dot represents the proportion of larvae that respond to each stimulus, which are delivered at 1-min interstimulus intervals (ISIs). Memory was evident at the re-test block 5 h after training, where larvae have not recovered to untrained levels (those in block 1). Arrows, 10$^{th}$ stimulus in each block.

See also Figure S1 and Videos S1 and S2.

response returned to near maximal levels but then decreased more rapidly, and to lower values, during subsequent training blocks. This is consistent with previous observations of long-term habituation, which often manifests as a faster rate of re-habituation [1]. Memory retention was tested in a "re-test" block 5 h after training (Figure 1C), which revealed that dark-flash responses did not recover to naive levels (those observed in the first block) but rather exhibited even greater reductions compared to the last block of training. We confirmed that this effect is not due to experimental time by comparing larvae that had undergone the 4-block training protocol with controls that had not been trained, either 5 or 28 h after the training period (Figure S1A). In both experiments, trained larvae responded less frequently, indicating these reductions are based on training experience, though by 28 h, there was a significant recovery toward untrained levels. Therefore, the habituation paradigm presented here induces memory that lasts robustly for 5 h, and effects are seen for up to 28 h.

Decreasing responsiveness is characteristic of habituation, but it is important to rule out fatigue as an alternative explanation. To that end, we monitored spontaneous movements (when no stimuli are delivered), the response to acoustic tap stimuli, and the ability of larvae to detect and respond to visual motion stimuli using the optomotor response (OMR) [23]. In each case, we did not detect reduced responses in the trained larvae compared to controls, indicating that fatigue, or a generalization of habituation to other behaviors, does not occur (Figures S1B–S1I). In fact, rather than a fatigue-induced reduction in motility, we observed small increases in displacement, turning rate, and acoustic tap responses after training, indicating that dark-flash habituation training may be slightly arousing to the animals. Importantly, as the OMR is also a retina-dependent behavior that depends on the detection of luminance transitions in the retina, and as the OMR is unaffected by our training protocol, we conclude that habituation does not affect vision globally. This furthermore indicates that habituation is unlikely to occur at the general sensory neuron (photoreceptor) level but rather selectively within the dark-flash response circuitry.

## Multiple Dark Flash Response Components Habituate

Habituation can be measured as a binary reduction in response (as above) or alternatively via decreases in the magnitude of the response [1]. To further analyze this process, we asked how many other aspects of the response habituate and, subsequently, how these might be related to one another. In total, we identified 8 components of the dark-flash response that habituate (Figures 2A–2H, and S2A).

(1) Probability of responding to the stimulus, as discussed above.

(2) Double responses: zebrafish larvae move in bouts, separated by periods of inactivity. By tracking behavior over the full 1 s of the dark flash, we observed that many larvae do not execute a single response but rather execute multiple large-angle turns separated by at least 50 ms of inactivity (Videos S2 and S3). The proportion of larvae executing at least two responses habituates (Figure 2B).

(3) Latency: consistent with previous results [15], we observed that the latency from the stimulus to the response habituates, increasing by an average of 197 ms (first stimulus versus last stimulus of block 4). Similar to components 1 and 2, we saw progressive accumulation of habituation across blocks, but retention after 5 h was not as robust, though it still remained habituated compared to naive levels (Figure 2C). We also note that, although acoustic responses can be parsed into kinematically distinct response types based on latency (short- and long-latency C-bends) [24], we do not observe a bimodal

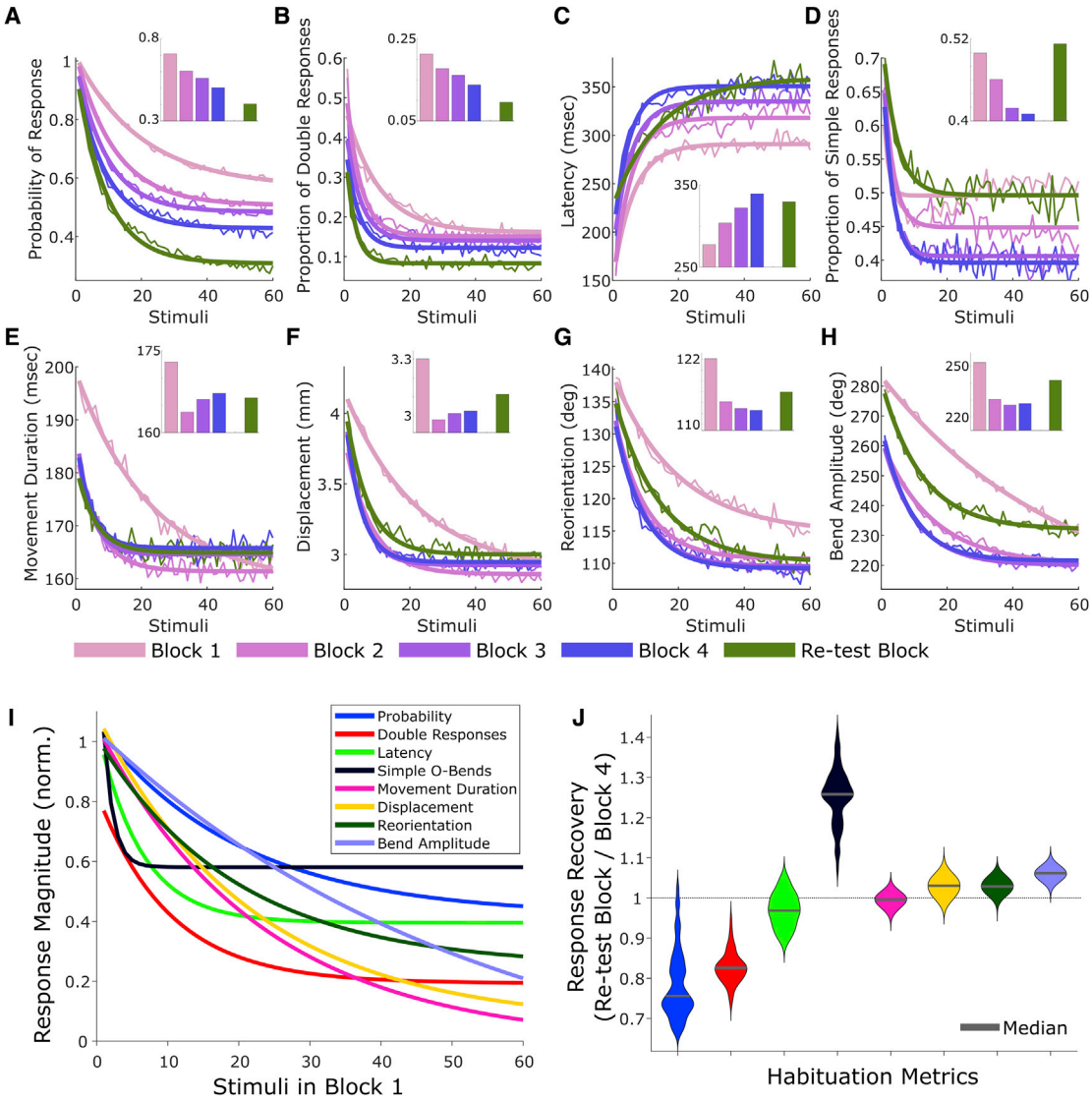


**Figure 2. Habituation Kinetics of Different Dark-Flash Response Components**

(A–H) Exponential fits of habituation curves for each of the 4 training blocks and the re-test block plotted overlapping in time, color coded by training block (thick line); thin line, raw data (mean across 3,120 larvae); insets, mean response per block, for (A) the probability of executing a dark-flash response, (B) the proportion of larvae executing at least two responses, (C) the latency from the stimulus to the initiation of the response (note that the latency values increase, indicating habituation), (D) the proportion of larvae executing a simple response, (E) the duration of the movement, (F) the displacement of the larvae, (G) the reorientation angle achieved by the movement, and (H) the maximal bend amplitude.

(I) Exponential fit curves for block 1 habituation performance plotted across components. Data were normalized such that initial response is equal to 1, and the minimal response observed in any flash is 0.

(J) Violin plots of the distributions of response recovery during the 5-h retention window, computed as the mean values across larvae for the trials in the re-test block, divided by those in the last training block (block 4). Values greater than 1 reflect a recovery of the response.

See also Figure S2 and Video S3.

distribution in the dark-flash response latencies, indicating such relationship does not exist for this response (Figure S2B).

(4) Proportion of simple responses: in response to a dark flash, some larvae perform multiple high-amplitude bends in the same direction followed by a swim, as opposed to the classic O-bend response that involves only one such bend before the swim. We term these "compound responses" and "simple responses," respectively (Figure S2C; Video S3). Before training, 61% of the responses are simple responses, which decreases to 41% with training (Figure 2D). We observed across-block habituation during training, but retention is poorer than components 1–3 and fully recovers to untrained levels after 5 h.

(5–8) We also observed habituation in dark-flash response components related to the kinematic magnitude of the

movement, including its (5) duration, (6) displacement, (7) reorientation, and (8) bend amplitude (Figures 2E–2H). Unlike components 1–4, habituation learning of these latter kinematic components occurred mostly during the first block and did not decrease appreciably after block 2. Memory in these components was retained after 5 h, with varying degrees of recovery.

These results demonstrate that the dark-flash response, rather than being an "all or nothing" response, is actually composed of multiple behavior components capable of adaptation during habituation. We noticed a significant degree of variability in learning and memory kinetics (Figures 2I and 2J), consistent with the idea that habituation of individual components, rather than resulting redundantly from a single mechanism, instead results from multiple mechanisms with differential kinetics of adoption and decay.

## Habituation Occurs at Multiple Circuit Loci

The differences in the kinetics of habituation that we have observed could still be explained by a single-site plasticity model, where plasticity occurs at a single locus that is upstream of multiple independent circuit branches. Differences in the synaptic and molecular makeup of these downstream branches could result in differential rates habituation. To further explore the separability of the components of dark-flash habituation, we took advantage of spontaneous variability present in our dataset. Namely, although the majority of individual larvae habituate, there is considerable spread in the learning distributions (Figure 3A). We reasoned that, if habituation occurs at a single-circuit locus, then the learning performance of the different response components would be correlated across larvae. In such a scenario, larvae would vary in their ability to habituate at this locus, but individual larvae would exhibit a consistent level of habituation across all behavior components. Alternatively, if habituation of individual behavior components occurs at distinct loci within the circuit, then learning performance should be independent of one another in any individual larva. Consequently, this should result in a lack of correlation in learning performance for individual components across larvae.

Our analysis indicates that both scenarios occur. We observed strong positive correlations between some components, such as displacement and movement duration (Figure 3B). These two components also show similar learning and retention kinetics (Figures 2I and 2J), further supporting the idea that they habituate through a single mechanism. However, other components, such as probability and movement duration showed no correlation (Figure 3C), demonstrating that the capacity of a larva to learn to respond less frequently is uncoupled from its ability to learn to respond with a shorter movement. Analysis of all pairwise comparisons (Figure 3D) revealed that learning was largely correlated across the kinematic components (5–8). Probability and double responses are also correlated, although latency and the proportion of simple responses are not strongly correlated to any other group. We also observed similar patterns when analyzing how correlated the different components are across fish when analyzing only the responses to the first flash (Figure S2D). This indicates that these components are separately regulated modules of behavior, and it is not the process of habituation alone that uncouples them. This leads us to conclude that the dark-flash response is composed of multiple separately regulated components and that plasticity exerted at four or more distinct loci acts to independently modulate these components during habituation.

We also observed weak negative correlations between habituation of some response components, most prominently between probability and bend amplitude (Figure 3E). One possible explanation for such subtle anti-correlations might be due to the circuit architecture of habituation. For example, if different plasticity loci in the circuit operate in parallel, we would expect to observe no correlation in learning performance for their respective components. Alternatively, if the loci are arranged in series, habituation at the upstream locus will reduce the amount of training signal that reaches the downstream locus. Because habituation results from repeated stimulation, this would result in a negative relationship between upstream plasticity and downstream training (Figure 3F). To demonstrate that this can occur, we modeled two habituating neurons connected in series. Both neurons acted as habituation loci with the same habituation kinetics, with random noise added to simulate learning variability. This simulation is in line with the idea that anti-correlated distributions manifest from such an architecture and that the magnitude of the anti-correlation increases with variability at the upstream plasticity locus (Figure 3G). If we assume from a sensorimotor perspective that the locus that habituates probability is upstream of bend amplitude, then this simple model predicts that the magnitude of the anti-correlations in habituation for probability and bend amplitude would increase with the variability for probability. Using iterative sub-sampling of groups of 100 larvae, we observed that, indeed, the magnitude of the anti-correlations increases along with the variance in percent habituation for probability (Figure 3H). Combined, these results support a model by which habituation results from distributed effects spread across multiple circuit loci, some of which operate in parallel in the circuit (no correlation in learning performance across larvae), and others operate in series, resulting in negative correlations.

## Habituation of Different Dark-Flash Response Components Is Molecularly Separable

Although our results indicate that multiple sites in the dark-flash response circuit exhibit plasticity independently during dark-flash habituation, it is unclear whether these distinct events use separate molecular pathways. If different molecular pathways operate, then it should be possible to identify manipulations that differentially affect different response components. To test this, we analyzed *neurofibromatosis 1* (*nf1*) mutants, which fail to habituate the latency of their dark-flash responses [15]. When we analyzed habituation in *nf1a;nf1b* double-homozygous (nf1) mutants, we found that not all components are equally affected (Figure 4A). In fact, although learning performance is strongly inhibited for latency (Figure 4B), learning performance is indistinguishable from controls for displacement (Figure 4C), strongly suggesting that individual components of dark-flash habituation are regulated via distinct molecular mechanisms. We note that *nf1* mutants also show alterations in the naive response to the first flash for some components, including a significantly longer latency (Figure S3). However, a lack of

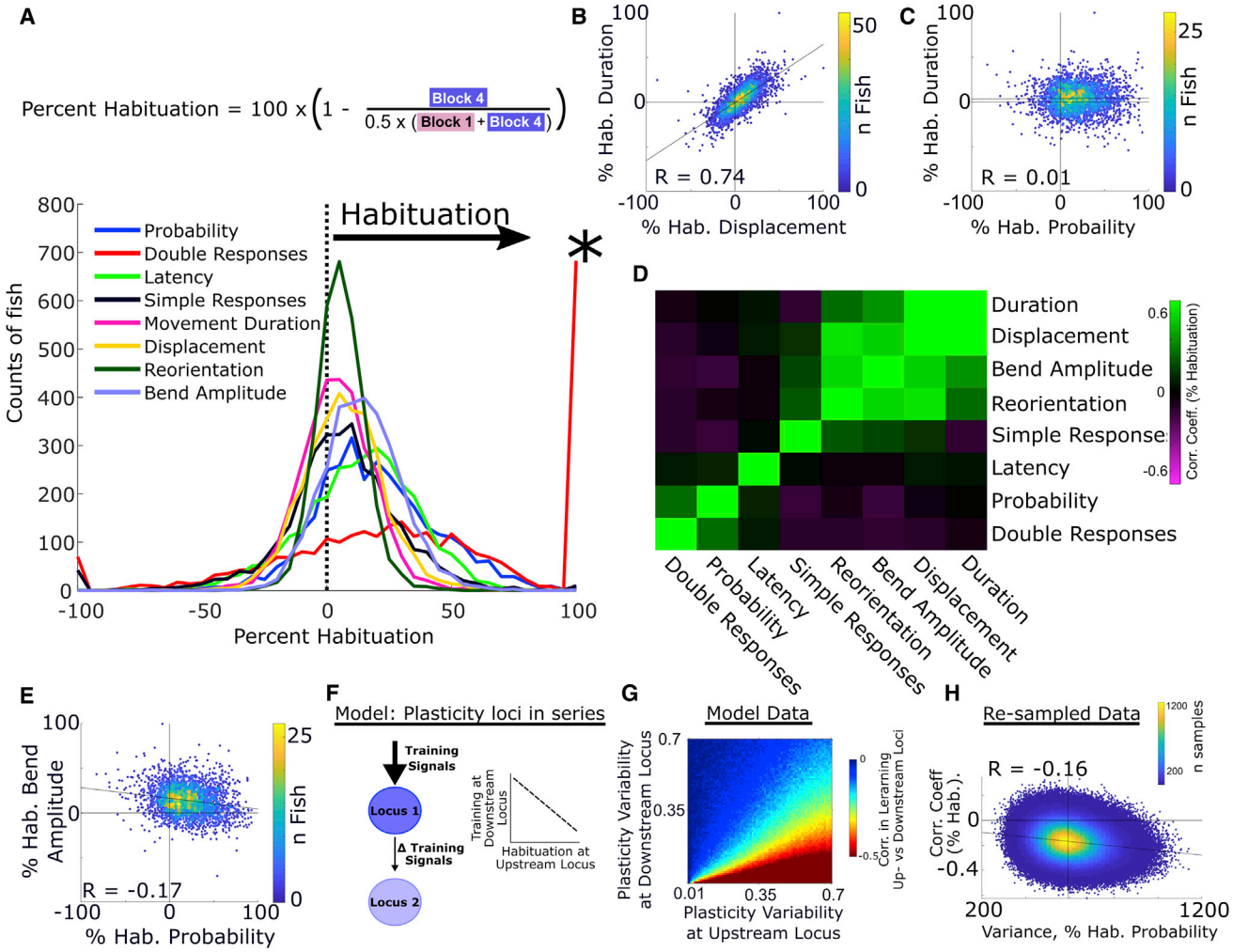


**Figure 3. Habituation of Different Response Components Occurs Independently**

(A) Percent habituation histograms of individual larvae across the 8 dark-flash response components (n = 3,120 larvae). Asterisk marks the uptick in double responses, reflecting the individuals that show 100% habituation.

(B) Scatterplots and correlation coefficient comparing percent habituation for the displacement and duration components. Color map reflects the density of points (R = 0.74; $p < 1 \times 10^{-10}$; Spearman's rho).

(C) Same analysis as (B), revealing the probability and duration components are not correlated (R = 0.01; p = 0.48; Spearman's rho).

(D) Hierarchically clustered correlation matrix (Spearman's rho), comparing percent habituation of the response components.

(E) Weak but significant anti-correlation observed between the bend amplitude and probability components ($R = -0.17$; $p < 1 \times 10^{-20}$, Spearman's rho).

(F) Conceptual model for how anti-correlations of habituation performance could arise. If two plasticity loci exist in series and are habituating, in larvae where habituation at the upstream locus is stronger than average, this would result in less than average habituation training at the downstream node and vice versa.

(G) Simulation results modeling plasticity at two loci that follow the kinetics of habituation for probability plus Gaussian noise. Training at the downstream locus depends on how much habituation occurs at the upstream node, resulting in anti-correlations in learning performance. The magnitude of the anti-correlations increases with learning variability at the upstream locus and decreasing variability at the downstream locus (n = 10,000 runs per comparison).

(H) Re-sampling of the original 3,200 larvae into random 100-larvae subsets over 2,000,000 iterations. Variance in percent habituation for probability scales with the magnitude of the anti-correlation between percent habituation for probability and bend amplitude ($p < 1 \times 10^{-10}$; Spearman's rho).

See also Figure S2D.

habituation for latency is not due to a ceiling effect, as sibling controls surpass mutant values during training (Figure 4B).

To further generalize these findings, we next performed a set of pharmacological manipulations. Due to their previously identified roles in zebrafish behavioral plasticity and habituation, we tested antipsychotic drugs that act as antagonists of the dopamine and serotonin systems [14, 24, 25]. Specifically, treatment with haloperidol, a dopamine D2 receptor antagonist, had a wide range of effects on habituation (Figure 4D). Remarkably, these effects include oppositely signed effects for different response components, such as increased habituation for latency (Figure 4E) and decreased habituation for bend amplitude (Figure 4F). Similarly, treatment with pimozide and clozapine, which also antagonize the dopamine D2 receptor, had separable effects across different behavior components (Figures 4G and 4H). These pharmacological experiments confirm that

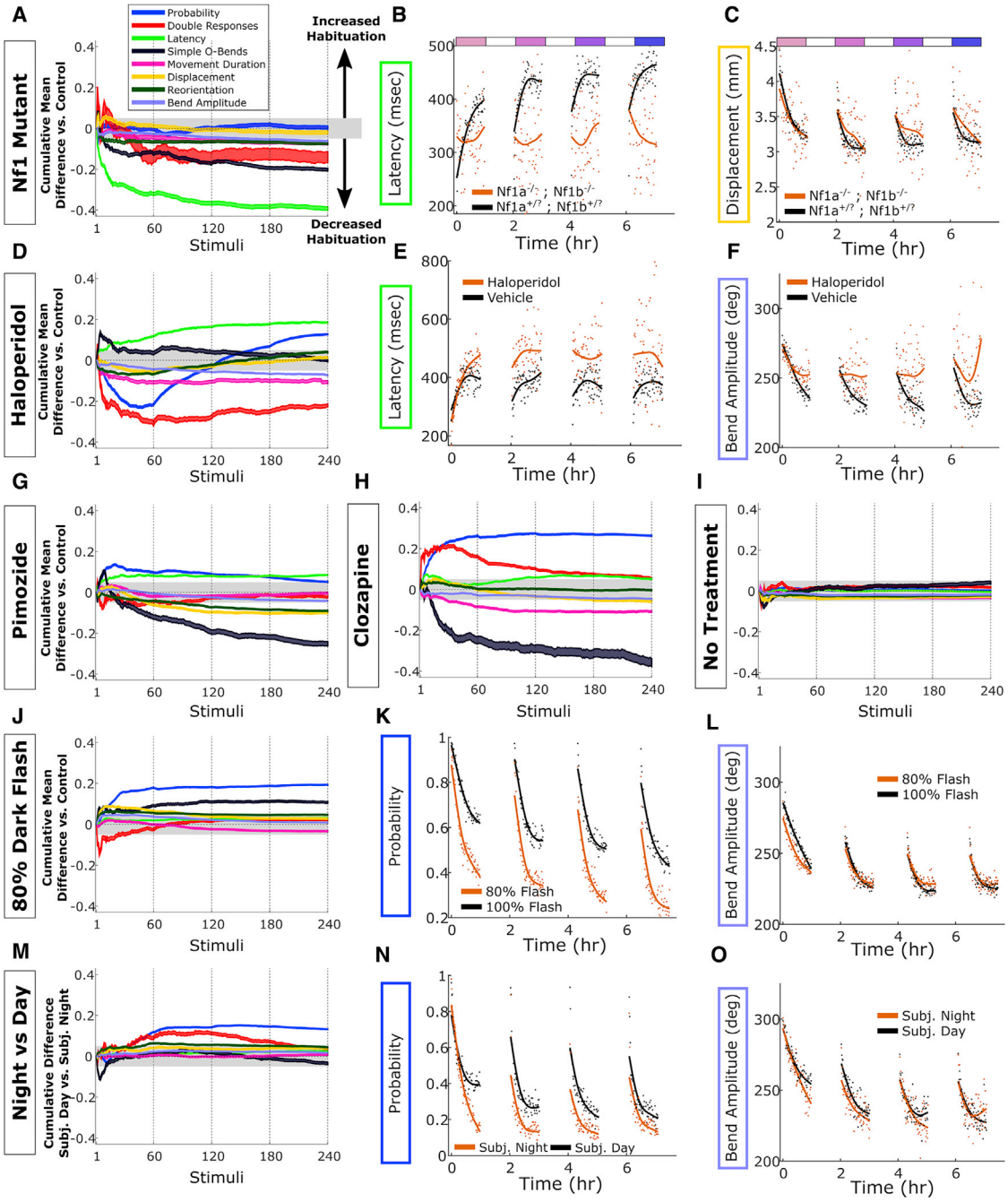


**Figure 4. Habituation of Different Response Components Is Separable Genetically, Pharmacologically, by Stimulus Strength and Circadian Phase**

(A) Cumulative plot of the differences in habituation rate for the response components. These plots display the cumulative average differences in the mean response across larvae of *nf1a;nf1b* double-homozygous mutants (n = 41 larvae) compared to sibling controls (n = 678 larvae). Difference from 0 reflects divergence in response across the 240 dark-flash stimuli in the 4 training blocks, with negative values reflecting a failure to habituate. The widths of the lines are bootstrapped 99.5% confidence intervals. The gray boxed region reflects the expected non-significant effect size from a negative control experiment (see I). Mutants fail to habituate some components, most profoundly for the latency metric.

(B) Raw data (dots, mean across larvae for each stimulus) and smoothing spline fits (solid lines), demonstrating that *nf1a;nf1b* double mutants fail to habituate when measuring latency (note that increasing latencies indicate habituation).

(C) *nf1a;nf1b* double mutants habituate normally when measuring displacement.

(D) Cumulative difference plots for treatment with haloperidol (10 μM; n = 80 larvae) versus vehicle controls (0.1% DMSO; n = 140 larvae).

(E and F) Treatment with haloperidol (E) increases habituation performance when measuring latency and (F) decreases habituation when measuring bend amplitude.

*(legend continued on next page)*

habituation of different response components occurs via different molecular mechanisms.

### Habituation of Different Response Components Is Separably Modulated by Stimulus Strength and the Circadian Rhythm

Although we have shown that habituation of different response components is independent, it was unclear what utility such independence might serve. We reasoned that having a modular system might allow an animal to adapt its behavior with more flexibility or specificity in different contexts. To test this, we first asked how habituation rates change when the stimulus is weakened. Instead of delivering a full dark flash, we decreased the illumination by only 80%. This weakened stimulus is still strong enough to reliably elicit responses (Figure S3F) [16] and causes the larvae to habituate more rapidly (Figures 4J–4L). However, the effect was selective for the probability component, and other components, including bend amplitude, showed much less modulation. This indicates that the nature of the stimulus can alter the habituation rate of different behavioral components in different ways.

Finally, to further test our hypothesis that a modular system enables animals to adapt habituation behavior in a more context-dependent manner, we compared habituation rates during different phases of the circadian rhythm. The circadian phase modulates the endogenous arousal level of zebrafish larvae [26] and may also alter the salience of a dark flash because darkness is an expected condition at night. Specifically, we raised a subset of larvae on a reversed light cycle and subjected them to our habituation assay together with their normally raised siblings. By testing the behavior of larvae during either their subjective day or their subjective night, we found that there was a circadian influence on habituation (Figures 4M–4O). Similar to the effect of a weakened stimulus, we identified selective effects on the habituation rate of the probability component, which showed significantly stronger habituation during the night phase. This could allow the larvae to more rapidly cease responding during the night, or to weaker dark flashes, while continuing to adapt kinematic-related components at the normal rate. Thus, modularity in habituation can allow for the adaptation of specific behavioral components based on both the context of the animal and the stimulus.

## DISCUSSION

Studies of habituation in several species have focused on identifying the site and underlying mechanism of plasticity. These efforts have generally associated habituation with plasticity in upstream sensory-related brain areas, including depression of the sensory-to-motor-neuron synapse in the *Aplysia* gill and siphon withdrawal reflex [5, 6], depression of the sensory-to-interneuron synapse in *C. elegans* [8], and enhanced GABAergic inhibition in olfactory glomeruli in the *Drosophila* antennal lobe [7]. However, one recent study in mice associated habituation to a visual stimulus with synaptic potentiation in the visual cortex, indicating that habituation does not occur via sensory depression in this system [10]. Although there is substantial data confirming the importance of these specific loci, it is possible that these individual sites are only one of many points in the circuit where plasticity is occurring.

The experiments presented here quantify behavior across thousands of larval zebrafish and demonstrate that dark-flash habituation occurs via multiple plasticity events, where each of these events acts to suppress a specific component of behavior. These different plasticity events manifest in differential kinetics of learning and forgetting and a lack of correlated learning across behavioral components. Particularly surprising was the separability of probability and latency, because in the simplest model, latency is a direct function of probability (as in a Poisson process, similar to [27]). Because the brain can adapt these two aspects of behavior separately, the decision of whether to respond to a stimulus appears to be uncoupled from the decision of when to respond. Although a previous study in bullfrogs found similar rates of habituation for different behavioral components in a population of animals [28], our method examined correlation of response component habituation within individuals and thus serves as a more direct test for a common underlying site of plasticity.

Our results indicate that the brain not only implements plasticity in multiple circuit loci but also does this via multiple molecular mechanisms. We found that some components of habituation require Nf1, and others do not. Furthermore, our experiments with antipsychotic drugs indicate that habituation of only a subset of components involves signaling through dopamine and/or serotonin receptors. This opens the path for a whole series of detailed investigations on the precise nature and mechanistic role of these pathways that will be the subject of future studies. However, as these drugs all antagonize the dopamine D2 receptor and all increase habituation for latency, it is likely that dopamine signaling negatively regulates this aspect of habituation. The effects of opposite sign that a single drug can have across different components suggest that the same molecular pathways are capable of influencing different plasticity events in oppositely signed manners. Alternatively, these effects may relate to the promiscuous nature of these drugs, which can

(G and H) Cumulative difference plots comparing 0.1% DMSO vehicle controls and after treatment with (G) pimozide (1 μM; n = 140 treated larvae; n = 160 controls) and (H) clozapine (10 μM; n = 120 treated larvae; n = 160 controls).

(I) Negative control experiment comparing wild-type larvae in the same experiment that are given no treatments (n = 150 larvae, both groups). These plots do not diverge consistently from ±0.05, which is taken as an empirically derived threshold for a meaningful effect size.

(J) Cumulative difference plots comparing larvae given an 80% dark flash (light intensity transitions from 100% to 20%), with larvae given a normal 100% dark flash (n = 300 larvae, both groups).

(K and L) Raw data (dots, mean across larvae for each stimulus) and smoothing spline fits (solid lines), showing how larvae habituate more rapidly to the weaker stimulus for the (K) probability component, while (L) habituating the bend amplitude similarly to controls.

(M) Cumulative difference plots comparing larvae in the subjective night phase of the circadian cycle with those in the subjective day (n = 150 larvae, both groups).

(N and O) Larvae in the subjective night phase show increased habituation performance for the (N) probability component and (O) much weaker effects on bend amplitude.

See also Figure S3.

affect many targets [29]. Considering that these drugs are used to treat schizophrenia and that there are well-established connections between habituation and schizophrenia (as well as other psychiatric disorders, including autism) [30, 31], our approach that allows disambiguating specific behavioral components in a high-throughput assay may have important relevance for translational approaches. For example, it might aid efforts aimed at identifying more selective therapeutic compounds that share targets with known beneficial pharmaceuticals but that act with greater molecular and behavior-modifying precision.

Habituation of different response components may result from plasticity at different synapses within the same neurons, but a more parsimonious mechanism would involve different neurons that are part of parallel or serial pathways within the circuit. The negative correlations in habituation performance that we observed in some components also support a model where plasticity occurs in different neurons that are arranged in sequence within a sensory motor path. This can be explained by a simple model, where individual variations in plasticity at upstream neurons result in variable levels of activation and thereby variable opportunity for habituation at downstream neurons. The physical location of plasticity sites remains to be determined. However, it is tempting to speculate that plasticity regulating the release of the dark-flash response, such as probability and latency, might exist more toward the earlier sensory-related parts of the circuit, and regulation of kinematic parameters might occur downstream toward the motor circuitry in the hindbrain or spinal cord.

In light of recent work in *C. elegans*, where multiple genetically separable mechanisms have been shown to underlie short-term habituation [11–13], we propose that such modularity is a conserved feature of habituation. Thus, to accurately identify and characterize the possible neural implementation of habituation, it is important to consider a movement bout not as a single behavioral output but rather as a combination of multiple independent modules. Additionally, although behavioral classification in larval zebrafish often considers the entire bout as the unit of behavior [17], these results suggest that sub-components of bouts may represent an important unit of behavior in this system. Similarly, in our analyses, we have treated all high-amplitude turns exhibited in response to a dark flash as a single "response type" or bout, which has multiple components that are modulated during habituation. Alternatively, it is possible that dark flashes elicit multiple distinct bout types with different neural circuit underpinnings (O-bends versus SATs [17]; the simple and complex responses we observe here) and that habituation acts to shift the proportions of bout types expressed. This question may be resolved when we have a better understanding of the circuit elements underlying response components or bout types.

Why might the zebrafish brain have evolved such a seemingly complex strategy to habituate? Perhaps plasticity to repeated stimulation is simply a pervasive adaptation at many synapses in a circuit, and we can observe these multiple effects when analyzing behavior in a multi-component manner. Alternatively, approaching habituation in a modular way would facilitate behavioral flexibility. This would allow for specific adaptations rather than a simple global reduction in responses, perhaps tuned based on brain state, stimulus, or environmental context. Indeed, we found that habituation of probability is modulated by the circadian rhythm and dark-flash intensity, and other response components are not. This demonstrates that habituation acts in a modular fashion to tune the habituation rate of different components of behavior based on context. Thus, our results reveal that the strategies taken by even relatively simple larval zebrafish brains to habituate require a surprisingly complex combination of independent plasticity events distributed across the circuit.

## STAR★METHODS

Detailed methods are provided in the online version of this paper and include the following:

- KEY RESOURCES TABLE
- CONTACT FOR REAGENT AND RESOURCE SHARING
- EXPERIMENTAL MODEL AND SUBJECT DETAILS
- METHOD DETAILS
  - Behavior recording
  - Multi-fish-tracker
  - Offline video tracking
  - Pharmacology
- QUANTIFICATION AND STATISTICAL ANALYSIS
  - Behavioral quantification
  - Modeling
- DATA AND SOFTWARE AVAILABILITY

## SUPPLEMENTAL INFORMATION

Supplemental Information can be found online at https://doi.org/10.1016/j.cub.2019.02.039.

## ACKNOWLEDGMENTS

We thank the Granato, Engert, and Schier lab members for helpful advice regarding the manuscript and work. This work was supported by the NIH grant RO1 MH109498 (M.G.) and the NIH Brain Initiative grants U19NS104653, R24 NS086601, and R43OD024879, as well as Simons Foundation grants SCGB nos. 542973 and 325207 (F.E.).

## AUTHOR CONTRIBUTIONS

Conceptualization, O.R., F.E., and M.G.; Methodology, O.R.; Software, M.H. and O.R.; Investigation, O.R.; Resources, H.S. and G.F.; Writing – Original Draft, O.R.; Writing – Review & Editing, O.R., M.H., H.S., A.F.S., F.E., and M.G.; Supervision, A.F.S., F.E., and M.G.; Funding Acquisition, F.E. and M.G.

## DECLARATION OF INTERESTS

The authors declare no competing interests.

Received: September 24, 2018
Revised: January 18, 2019
Accepted: February 15, 2019
Published: April 4, 2019

## REFERENCES

1. Rankin, C.H., Abrams, T., Barry, R.J., Bhatnagar, S., Clayton, D.F., Colombo, J., Coppola, G., Geyer, M.A., Glanzman, D.L., Marsland, S., et al. (2009). Habituation revisited: an updated and revised description of the behavioral characteristics of habituation. Neurobiol. Learn. Mem. *92*, 135–138.

2. Glanzman, D.L. (2009). Habituation in Aplysia: the Cheshire cat of neurobiology. Neurobiol. Learn. Mem. *92*, 147–154.
3. Bailey, C.H., Kandel, E.R., and Harris, K.M. (2015). Structural components of synaptic plasticity and memory consolidation. Cold Spring Harb. Perspect. Biol. *7*, a021758.
4. Kandel, E.R. (2001). The molecular biology of memory storage: a dialogue between genes and synapses. Science *294*, 1030–1038.
5. Pinsker, H., Kupfermann, I., Castellucci, V., and Kandel, E. (1970). Habituation and dishabituation of the gill-withdrawal reflex in Aplysia. Science *167*, 1740–1742.
6. Bailey, C.H., and Chen, M. (1988). Long-term memory in Aplysia modulates the total number of varicosities of single identified sensory neurons. Proc. Natl. Acad. Sci. USA *85*, 2373–2377.
7. Das, S., Sadanandappa, M.K., Dervan, A., Larkin, A., Lee, J.A., Sudhakaran, I.P., Priya, R., Heidari, R., Holohan, E.E., Pimentel, A., et al. (2011). Plasticity of local GABAergic interneurons drives olfactory habituation. Proc. Natl. Acad. Sci. USA *108*, E646–E654.
8. Rose, J.K., Kaun, K.R., Chen, S.H., and Rankin, C.H. (2003). GLR-1, a non-NMDA glutamate receptor homolog, is critical for long-term memory in Caenorhabditis elegans. J. Neurosci. *23*, 9595–9599.
9. Tomsic, D., Berón de Astrada, M., and Sztarker, J. (2003). Identification of individual neurons reflecting short- and long-term visual memory in an arthropodo. J. Neurosci. *23*, 8539–8546.
10. Cooke, S.F., Komorowski, R.W., Kaplan, E.S., Gavornik, J.P., and Bear, M.F. (2015). Visual recognition memory, manifested as long-term habituation, requires synaptic plasticity in V1. Nat. Neurosci. *18*, 262–271.
11. Ardiel, E.L., Yu, A.J., Giles, A.C., and Rankin, C.H. (2017). Habituation as an adaptive shift in response strategy mediated by neuropeptides. npj Science of Learning *2*, 9.
12. Ardiel, E.L., Giles, A.C., Yu, A.J., Lindsay, T.H., Lockery, S.R., and Rankin, C.H. (2016). Dopamine receptor DOP-4 modulates habituation to repetitive photoactivation of a C. elegans polymodal nociceptor. Learn. Mem. *23*, 495–503.
13. Ardiel, E.L., McDiarmid, T.A., Timbers, T.A., Lee, K.C.Y., Safaei, J., Pelech, S.L., and Rankin, C.H. (2018). Insights into the roles of CMK-1 and OGT-1 in interstimulus interval-dependent habituation in *Caenorhabditis elegans*. Proc. Biol. Sci. *285*, 20182084.
14. Wolman, M.A., Jain, R.A., Liss, L., and Granato, M. (2011). Chemical modulation of memory formation in larval zebrafish. Proc. Natl. Acad. Sci. USA *108*, 15468–15473.
15. Wolman, M.A., de Groh, E.D., McBride, S.M., Jongens, T.A., Granato, M., and Epstein, J.A. (2014). Modulation of cAMP and ras signaling pathways improves distinct behavioral deficits in a zebrafish model of neurofibromatosis type 1. Cell Rep. *8*, 1265–1270.
16. Burgess, H.A., and Granato, M. (2007). Modulation of locomotor activity in larval zebrafish during light adaptation. J. Exp. Biol. *210*, 2526–2539.
17. Marques, J.C., Lackner, S., Félix, R., and Orger, M.B. (2018). Structure of the zebrafish locomotor repertoire revealed with unsupervised behavioral clustering. Curr. Biol. *28*, 181–195.e5.
18. Fernandes, A.M., Fero, K., Arrenberg, A.B., Bergeron, S.A., Driever, W., and Burgess, H.A. (2012). Deep brain photoreceptors control light-seeking behavior in zebrafish larvae. Curr. Biol. *22*, 2042–2047.
19. Huang, K.-H., Ahrens, M.B., Dunn, T.W., and Engert, F. (2013). Spinal projection neurons control turning behaviors in zebrafish. Curr. Biol. *23*, 1566–1573.
20. Orger, M.B., Kampff, A.R., Severi, K.E., Bollmann, J.H., and Engert, F. (2008). Control of visually guided behavior by distinct populations of spinal projection neurons. Nat. Neurosci. *11*, 327–333.
21. Costa, R.M., Federov, N.B., Kogan, J.H., Murphy, G.G., Stern, J., Ohno, M., Kucherlapati, R., Jacks, T., and Silva, A.J. (2002). Mechanism for the learning deficits in a mouse model of neurofibromatosis type 1. Nature *415*, 526–530.
22. Ho, I.S., Hannan, F., Guo, H.-F., Hakker, I., and Zhong, Y. (2007). Distinct functional domains of neurofibromatosis type 1 regulate immediate versus long-term memory formation. J. Neurosci. *27*, 6852–6857.
23. Portugues, R., and Engert, F. (2009). The neural basis of visual behaviors in the larval zebrafish. Curr. Opin. Neurobiol. *19*, 644–647.
24. Burgess, H.A., and Granato, M. (2007). Sensorimotor gating in larval zebrafish. J. Neurosci. *27*, 4984–4994.
25. Halberstadt, A.L., and Geyer, M.A. (2009). Habituation and sensitization of acoustic startle: opposite influences of dopamine D1 and D2-family receptors. Neurobiol. Learn. Mem. *92*, 243–248.
26. Hurd, M.W., and Cahill, G.M. (2002). Entraining signals initiate behavioral circadian rhythmicity in larval zebrafish. J. Biol. Rhythms *17*, 307–314.
27. Portugues, R., Haesemeyer, M., Blum, M.L., and Engert, F. (2015). Whole-field visual motion drives swimming in larval zebrafish via a stochastic process. J. Exp. Biol. *218*, 1433–1443.
28. Bee, M.A. (2003). Experience-based plasticity of acoustically evoked aggression in a territorial frog. J. Comp. Physiol. A Neuroethol. Sens. Neural Behav. Physiol. *189*, 485–496.
29. Wishart, D.S., Feunang, Y.D., Guo, A.C., Lo, E.J., Marcu, A., Grant, J.R., Sajed, T., Johnson, D., Li, C., Sayeeda, Z., et al. (2018). DrugBank 5.0: a major update to the DrugBank database for 2018. Nucleic Acids Res. *46* (D1), D1074–D1082.
30. Ramaswami, M. (2014). Network plasticity in adaptive filtering and behavioral habituation. Neuron *82*, 1216–1229.
31. McDiarmid, T.A., Bernardos, A.C., and Rankin, C.H. (2017). Habituation is altered in neuropsychiatric disorders-A comprehensive review with recommendations for experimental design and analysis. Neurosci. Biobehav. Rev. *80*, 286–305.
32. Shin, J., Padmanabhan, A., de Groh, E.D., Lee, J.-S., Haidar, S., Dahlberg, S., Guo, F., He, S., Wolman, M.A., Granato, M., et al. (2012). Zebrafish neurofibromatosis type 1 genes have redundant functions in tumorigenesis and embryonic development. Dis. Model. Mech. *5*, 881–894.
33. Schindelin, J., Arganda-Carreras, I., Frise, E., Kaynig, V., Longair, M., Pietzsch, T., Preibisch, S., Rueden, C., Saalfeld, S., Schmid, B., et al. (2012). Fiji: an open-source platform for biological-image analysis. Nat. Methods *9*, 676–682.
34. Hoffmann, H. (2015). violin.m - Simple violin plot using matlab default kernel density estimation. https://www.mathworks.com/matlabcentral/fileexchange/45134-violin-plot.

# STAR★METHODS

## KEY RESOURCES TABLE

| REAGENT or RESOURCE | SOURCE | IDENTIFIER |
|---|---|---|
| Chemicals, Peptides, and Recombinant Proteins | | |
| Haloperidol | Sigma | H1512 |
| Pimozide | Sigma | P1793 |
| Clozapine | Sigma | C6305 |
| Experimental Models: Organisms/Strains | | |
| Zebrafish: (Tupfel Long Fin, TL) wild type | https://zfin.org | https://zfin.org/ZDB-GENO-990623-2 |
| Zebrafish: *nf1a*$^{p301}$ | [32] | http://zfin.org/ZDB-ALT-130528-1 |
| Zebrafish: *nf1b*$^{p303}$ | [32] | http://zfin.org/ZDB-ALT-130528-3 |
| Oligonucleotides | | |
| Proprietary primers for KASP genotyping of *nf1a*$^{p301}$ and *nf1b*$^{p303}$ alleles | LGC Genomics | N/A |
| Software and Algorithms | | |
| MATLAB R2018a | Mathworks | https://www.mathworks.com/ |
| FIJI | [33] | https://fiji.sc/ |
| Multi-fish-tracker | This paper, C# | Upon request |

## CONTACT FOR REAGENT AND RESOURCE SHARING

Further information and requests for resources and reagents should be directed to and will be fulfilled by the Lead Contact, Michael Granato (granatom@pennmedicine.upenn.edu).

## EXPERIMENTAL MODEL AND SUBJECT DETAILS

Experiments were conducted on 5-6 dpf larval zebrafish (*Danio rerio*, TLF strain) raised in E3 medium at 29°C on a 14:10 hr light cycle. For each experiment, larvae from multiple clutches (5-20 mating pairs) were collected, and the clutch populations were mixed evenly between treatment and control groups during experiments. For the circadian experiments (Figures 4J–4L), larvae tested in the subjective day were raised on a 9am-ON, 11pm-OFF light cycle, while larvae tested in the subjective night were raised on an 9pm-ON, 11am-OFF light cycle, and both groups were tested beginning at ~12:30pm. Breeding adult zebrafish were maintained at 28°C. Behavioral assays on larvae carrying mutations for Nf1a$^{p301}$ (ZDB-ALT-130528-1) and Nf1b$^{p303}$ (ZDB-ALT-130528-3) were conducted blind to genotype. Subsequent genotyping was performed with the KASP method with proprietary primer sequences (LGC Genomics). This method was validated using previously described PCR genotyping [32]. All animal protocols were approved by the University of Pennsylvania Institutional Animal Care and Use Committee (IACUC).

## METHOD DETAILS

### Behavior recording

Larval behavior was recorded in multiwell plates fabricated from 6.3mm thick clear acrylic sheets (US Plastics). The acrylic was cut with a laser cutter into 8mm diameter wells with a volume of ~300 uL, arranged in a 20x15 grid for a total 300-well plate. 3.2mm white acrylic (US Plastics) was bonded to the cut wells (SciGrip 4), acting as both the bottom of the plate and the light diffuser. To minimize evaporation and to maintain a consistent ~28°C temperature in the behavior wells, the 300-well plate was placed under a 29-31°C water bath that acted as a heated lid for the plate.

Larvae were illuminated from below with IR LEDs (890nm, Vsiahy.com part number TSHF5410) driven by a 1A Buckpuck driver (Luxdrive). Images were recorded from above with EoSens 4CXP Monochrome Camera (Mikroton), an 85mm 1.8 AF D lens (Nikon) with a IR long-pass filter (LP780-62, Midwest optics), and a Cyton Quad Channel CoaXPress Frame Grabber (Bitflow). The camera was triggered at 560hz using a Teensy 3.2 microcontroller (PJRC).

Due to the symmetrical design of the behavioral assay (1 hr training blocks, 1 hr rest between blocks), we were able to double the throughput of the rig by alternatingly imaging between two separate 300-well plates during the experiment. The larvae in plate 1 were recorded during training, and during the rest period the camera view was switched to plate 2, which was trained and recorded during the rest period for plate 1 (and vice versa). Therefore, the experimental time for the first and second plates are offset by one hour.

Therefore, for the comparisons of trained and untrained larvae (Figure S1), the untrained larvae are always tested 1 hour after the trained larvae, and have been inside the rig for one hour longer. Switching the camera views was done by placing the camera at a 90 degree angle above the behavior plates and using two 4'' x 5'' 45-degree incidence hot mirrors (43-958, Edmund Optics) to direct the camera view toward the two behavior plates. The mirrors were attached to Nema 17 stepper motors (ROB-09238, Sparkfun), driven by an EasyDriver (ROB-12779, Sparkfun), a Teensy 3.2 microcontroller (PJRC), and the Multi-fish-tracker software. In this way they could be rotated in and out of place to view each plate. Light cross talk between the behavior plates was minimized using blackout hardboard (TB4, Thorlabs).

For visual stimuli, we made a rectangular ring of 115 RGB LEDs (WS2812B 5050 RGB LED Strip 1M 144LED/M, https://www.ebay.com) to border the 300-well plate, diffused by 3.2mm white acrylic (US Plastics). LEDs were controlled using a Teensy 3.2 microcontroller and the fastLED Animation library (http://fastled.io/). The LEDs were set to white color with a brightness value of 50, yielding an intensity of approximately 130uW/cm$^2$ at the behavior plate. During a dark flash, the LEDs were turned off for 1 s and video of larval responses was recorded at 560 Hz. After this, the light intensity increased linearly to the original brightness over 20 s. To induce the optomotor response, a translating stimulus was generated by illuminating every 8th LED along the top and bottom of the plate. The position of the illuminated LED was progressively shifted down the strip by ramping down the intensity of the illuminated LED, while ramping up the intensity of the adjacent LED. This results in a stimulus that is approximately sinusoidal in space, 5.5 cm peak to peak, translating at 5.5 cm per second. In this way, the motion stimuli were translated in the leftward and rightward directions relative to the plate, moving with a constant speed. The direction of motion was switched every 30 s, for a total testing period of 1 hour. The orientation of the zebrafish larvae was tracked online using the Multi-fish-tracker (see below) at 28 Hz and was used to quantify the optomotor response, which follows the direction of perceived motion. Acoustic tap stimuli were delivered using a Solenoid (ROB-10391, Sparkfun) that delivered a single tap to the top of the water bath and induced acoustic escape responses.

### Multi-fish-tracker

The code to track individual zebrafish larvae in a multi-well format was custom written in C# (Microsoft, USA) using Intel's integrated performance primitives (IPP, Intel, USA) for fast image processing. Specifically, a running average background was kept for each plate that was updated with an exponential decay time of 2 minutes. This was done to flexibly adapt to different lighting conditions. The plate was subsequently divided into two sections, which were tracked on separate threads to increase throughput. Individual wells were identified using user-defined masks. The background was subtracted from each image and the resulting absolute difference was thresholded. Subsequently, the biggest object in each well, physically close to a previously identified larval position, was designated as the larval object, and relevant parameters such as position and heading angle were extracted using image moments. At baseline, tracking was performed at 28 Hz. For one second after each dark flash (or tap), all frames at the full camera frame-rate of 560 Hz were written to disk, for detailed offline kinematic analysis of behavior.

### Offline video tracking

Offline tracking on recorded videos was performed in MATLAB (Mathworks). The image was background subtracted and thresholded to identify the centroid of the larvae in each well. The background subtracted image was convolved with a disk filter with a 3 pixel radius, and the maximum intensity pixel was used to identify the head coordinate between the two pigmented eyes. To track the points along the body axis, we calculated a search direction vector defined by the head-to-centroid direction, and searched in an pi/3 sized arc placed at a radius of 5 pixels away from the head coordinate. The brightest point on this arc was considered the 2nd point along the fish. The search direction vector was then updated to the 1st to 2nd point direction, and a second arc was calculated 5 pixels from the 2nd point and the brightest pixel on this arc was assigned as the 3rd point. This process was iterated until 8 points were placed along the larvae. If no pixels above an intensity value of 4 were identified on an arc, tracking on this frame was stopped. The head coordinate was used to calculate displacement of the larvae, the head-to-centroid vector was used to calculate the heading orientation of the larvae, and the cumulative angle between the tail points was used to calculate the bend amplitude of the larvae.

### Pharmacology

Stock solutions of 100uM Haloperidol (H1512, Sigma), Pimozide (P1793, Sigma) and Clozapine (C6305, Sigma) were prepared in DMSO. 10x solutions in 1% DMSO in E3 media were then prepared, and 30uL of these 10x solutions were directly pipetted into the wells containing the larvae, which have a total volume of ~300uL, yielding 10uM Haloperidol, 1uM Pimozide, or 10uM Clozapine, in 0.1% DMSO vehicle. 30uL of 1% DMSO in E3 solution was pipetted into the vehicle control wells, yielding 0.1% DMSO vehicle control treated larvae. Larvae were treated with drug for between 30 and 90 minutes before the first dark flash was delivered. Vehicle control and drug treated larvae for each comparison were from the same clutches of larvae, and were assayed in different wells in the same behavioral plate.

## QUANTIFICATION AND STATISTICAL ANALYSIS

### Behavioral quantification

Analyses of larval behavior and statistical analyses were performed in MATLAB (Mathworks). For each dark flash or tap stimulus, the offline tracked videos were used to score behavior during the 1 s of recorded video. Dark flash responses were identified as

movement events that had a bend amplitude greater than 3 radians (172 degrees). Responses to taps were identified with a bend amplitude greater than 1 radian. Compound responses (Figure S2C) were classified as dark flash responses which had at least two local maxima in the bend amplitude trace during the initial bend before the bend amplitude trace crossed 0.

The proportion of the larval population that performed a response at each dark flash was used to quantify habituation performance for probability (Figures 1C and 2A). To generate habituation curves for the other behavioral components (Figures 2B–2I and S2A), larvae that did not perform an response for a given stimulus were excluded from the analysis at that stimulus. To fit exponential curves to each training block of 60 flashes ($x$), we used MATLAB's 'fit' function, with a 'fittype' formula of:

$$y = a \times 2^{-b \times x} + c \quad \text{(Equation 1)}$$

To quantify the recovery of the response in the population (Figure 2J), we averaged the response at each flash in Block 4 and the Re-test block across all larvae, and divided the Re-test block responses by the responses in Block 4. These distributions were plotted with 'violin.m' [34], with a bandwidth of 0.15. The comparison in dark flash responsiveness in trained and untrained larvae (Figure S1A) was performed by averaging the response for each population at each of the 60 dark flash stimuli, dividing the trained mean vector by the untrained mean vector, and plotting a histogram of the result. Values below 1 indicate suppressed responsiveness in the trained larvae.

Percent habituation was calculated for each larva as the decreased mean responsiveness for the 60 flashes in training Block 4, relative to the mean response for the 60 flashes training Block 1, using Equation 2. To make the distributions comparable across the different components of behavior, the minimum observed mean value across all larvae was subtracted from the block 1 and block 4 mean responses. This ensures that the responses can scale all the way to 0 regardless of behavior component -for example bend amplitude which by our definition of dark flash responses, must be at minimum 3 radians. Except when calculating for the probability behavior component, larvae that did not respond to a given stimulus were excluded from the analysis at that stimulus.

$$\%Habituation = 100 \times \left(1 - \frac{Block\ 4}{0.5 \times (Block\ 4 + Block\ 1)}\right) \quad \text{(Equation 2)}$$

For the correlational analyses of habituation performance for different dark flash response components across fish (Figures 3B–3E), the percent habituation scores for each component were assembled into a vector across the 3120 fish, and the spearman correlation coefficient was calculated using MATLAB's 'corr' function. The same was done for the naive response (Figure S2D), using the response to the first flash rather than percent habituation. This analysis can not be done comparing to the probability component, since the other components only manifest if a response actually occurs, as is reflected in the missing data in the matrix.

Analysis of stimulus-free swimming behavior (Figures S1F–S1H) was done using the online tracked larval coordinates from the Multi-fish-tracker. This was done for a 30 min period beginning one hour after the fourth dark flash habituation training block. Analysis of the optomotor response (OMR, Figures S1B–S1D), was done using the heading angle from the Multi-fish-tracker for one hour, beginning 3 hours after the fourth dark flash habituation training block. To calculate OMR performance, we isolated each 30 s period where the larvae were either being stimulated with leftward or rightward motion. We isolated the left-right component of the orientation by calculating the arcsin of the sin of the larval orientation. We then reflected the traces in time during the rightward stimulus presentation, such that each 30 s period would have an increasing slope if the larva were to reorient to follow the direction of motion (Figure S1D). All the 30 s periods were then averaged for each larva, and these averaged traces were fit with linear regression using MATLAB's 'polyfit' function. The slope of this fit (OMR slope) was taken as the measure for OMR performance for each larva (Figure S1E).

To calculate the cumulative difference in habituation performance for the Nf1 mutants, pharmacological treatments, 80% flash, and the circadian experiments (Figure 4), we calculated the average response across larvae at each dark flash. This was done for the treatment and control groups, yielding a mean vector for each group. These two vectors were normalized by dividing them by the initial response to the first flash for each group, and they were then subtracted, yielding a mean difference vector between stimulus and controls at each flash, from which we calculated the cumulative mean distribution. To generate statistical confidence in these distributions, we used bootstrapping of 2000 replicates, and calculated the 99.5% confidence intervals using MATLAB's 'fitdist' and 'paramci' functions. If the two groups are habituating similarly, then the difference vectors will have a mean of approximately 0, and thus the cumulative mean distribution would remain near 0. However, treatments that affect habituation will show strong increasing or decreasing cumulative mean distributions, reflecting increased or decreased habituation performance throughout training, respectively. We confirmed this by comparing larvae in even and odd numbered wells, which showed little divergence from 0 in the cumulative distributions (Figure 4I), and based on this dataset, we set a magnitude threshold of ± 0.05 reflecting the expected variability in this analysis.

## Modeling

We modeled two habituation loci acting in series in MATLAB. We began with the upstream locus, which follows learning kinetics of the exponential fit for the first training block of 60 flashes when measuring probability (Figure 2A, Block 1, Equation 1). In each model run, Gaussian noise was added to the coefficients of the fit, resulting in variable habituation curves. Each learning curve was normalized such that the maximum value is equal to 1. The downstream locus follows the same learning kinetics, but the learning curve was truncated based on how much habituation occurred at the upstream locus. This was measured as the area under the habituation

curve at the upstream node. If little habituation occurs, this will be close to 60, for the full 60 flashes. However, if habituation is profound this will approach 1. Therefore, the opportunity for habituation at the downstream node is negatively dependent on habituation performance at the upstream node. The variability in habituation across runs (axes in Figure 3G) was controlled by varying the standard deviation of the Gaussian distribution from which the noise added to the coefficients was derived. Learning performance was defined as in Equation 2, replacing Block 1 with the initial value of the habituation curve, and Block 4 with the final value of the curve. For each value of habituation variability ('sigma') at each locus, 10000 iterations of the model were run. The correlation in learning performance at each node across model runs (Spearman's rho) was calculated using MATLAB's 'corr' function.

## DATA AND SOFTWARE AVAILABILITY

C# and MATLAB code for tracking and behavioral analyses, Arduino code for delivering stimuli, and laser cutting templates are available upon request.